Since January 2020 Elsevier has created a COVID-19 resource centre with free information in English and Mandarin on the novel coronavirus COVID-19. The COVID-19 resource centre is hosted on Elsevier Connect, the company's public news and information website.

Applied Mathematics and Computation 226 (2014) 83–100

Contents lists available at ScienceDirect

Applied Mathematics and Computation

journal homepage: www.elsevier.com/locate/amc

Diseased prey predator model with general Holling type interactions

Banshidhar Sahoo *, Swarup Poria

Department of Applied Mathematics, University of Calcutta, Kolkata, West Bengal, India

ARTICLE INFO

Keywords:
General Holling
Disease
Permanence
Stability
Bifurcation
Hopf point

ABSTRACT

Choice of interaction function is one of the most important parts for modelling a food chain. Many models have been proposed as a diseased-prey predator model with Holling type-I or type-II or type-III interactions, but there is no model with general Holling type interactions. In this paper, we study a diseased prey–predator model with general Holling type interactions. Local stability conditions of equilibrium points are derived. We obtain the permanence and impermanence conditions of the system. The conditions for global stability of the system are also derived. The system exhibits limit cycle, period-2, higher periodic oscillations and chaotic behaviour for different values of Holling parameters. One parameter bifurcation analysis is done with respect to general Holling parameters and infection rate. We utilize the MATCONT package to analyse the detailed bifurcation scenario as the two important interaction parameters are varied. It is interesting to note that a diseased system becomes a disease free system for proper choice of interaction functions. Our results give an idea for constructing a realistic food chain model through proper choice of general Holling parameters.

1. Introduction

Mathematical models are increasingly used to guide public health policy decisions and to control infectious disease. Epidemic dynamics is an important method of studying the spread of infectious disease qualitatively and quantitatively. The research results are helpful to predict the developing tendency of the infectious disease, to determine the key factors of the spread of infectious disease and to seek the optimum strategies of preventing and controlling the spread of infectious diseases. Mathematical models have a long history in infectious disease ecology starting with Bernoulli's [1] modelling of smallpox and including Ross's [2] analysis of malaria. The earliest attempt to provide a quantitative understanding of the dynamics of malaria transmission was that of Ross [2]. Ross models consisted of a few differential equations to describe changes in densities of susceptible and infected people, and susceptible and infected mosquitoes. Based on his modelling, Ross introduced the concept of a threshold density and concluded that 'in order to counteract malaria anywhere we need not vanish Anopheles there entirely we need only to reduce their numbers below a certain figure [3]. Classical papers of mathematical modelling of infectious disease was constructed by Kermack and McKendrick (1927 [4], 1932 [5], and 1933 [6]). These papers had a major influence on the development of mathematical models for disease spread and are still relevant in many epidemic situations. Aim of ecological modelling is to understand the prevalence and distribution of a species, together with the factors that determine incidence, spread, and persistence (Anderson and May [7]; May and Anderson [8]; Bascompte and Rodriguez-Trelles [9]). Now we have models for many of the most important human emerging infectious dis-

* Corresponding author.
E-mail addresses: banshivu@gmail.com (B. Sahoo), swarup_p@yahoo.com (S. Poria).

0096-3003/$ - see front matter © 2013 Elsevier Inc. All rights reserved.
http://dx.doi.org/10.1016/j.amc.2013.10.013

eases e.g., HIV (May and Anderson [10]), malaria (Aron and May [11]; Macdonald [12]), SARS-coronavirus (Anderson et al. [13]), rabies (Murray and Seward [14]), and influenza (Ferguson and Anderson [15]). Mathematical models are also being used to explore wildlife disease dynamics (Grenfell and Dobson [16]; Hudson et al. [17]) and possible routes of zoonotic disease emergence. Understanding disease dynamics across hosts is an essential first step in understanding and articulating those conditions under which new diseases can emerge from wildlife reservoirs [18]. A predator–prey system with infected prey in polluted environment is proposed by Sinha et al. [19]. Anderson and May [20] were probably the first who considered the disease factor in a predator–prey dynamics and found that the pathogen tends to destabilize the predator–prey interaction. In Rosenzweig prey-predator model, Hadeler and Freedman [21] determined a threshold above which an infected equilibrium or an infected periodic solution appear. Chattopadhyay and Arino [22] considered a three species ecoepidemiological model and studied local stability of equilibrium points, extinction criteria of species and found condition for Hopf-bifurcation in an equivalent two-dimensional model. Haque and Chattopadhyay [23] studied the role of transmissible diseases in a prey dependent predator–prey system with prey infection. Haque and Venturino reported the influence of transmissible disease in prey taking Holling–Tanner predator–prey model [24]. The dynamical behaviour of the predator–prey system was investigated when a predator avoids infected prey and the predator has alternative sources of food ([25,26]). Bhattacharyya et al. [27] proposed a epidemiological model with nonlinear infection incidence. Das et al. [28] modified the HP model by introducing disease in the prey population. They derived conditions for population extinction and the conditions for permanent or impermanent of the system. Sahoo and Poria described a diseased prey-predator model supplying additional food to predator for biological control[29]. Recently, Haque et al. investigated predator-infected eco-epidemics systems with different functional responses[30].

In this paper, we modify the model of Das et al. [28] by introducing the general Holling type interactions in Section 2. Some preliminary results are derived in Section 3. In Section 4, the conditions for local stability of equilibrium points are derived. We derive the permanency and impermanence conditions for the model in Section 5. Section 6 presents the conditions for global stability. Section 7 contains the numerical simulation results of the model. We have done bifurcation analysis of the model with respect to general Holling parameters and have also investigated the influence of infection rate on the dynamics. The different routes of continuation of the associated bifurcations are analysed with the help of MATCONT software package ([31–33]).

2. Model formulation

All food chain models use some realistic interaction functions between preys and predators based on some biological hypothesis. A realistic interaction function should not allow the predators to grow arbitrarily fast, if prey is abundant. Apart from these basic biological considerations, Holling interaction functions are taken as simplest realistic interactions. Holling type-II function is defined as $F(X) = \frac{AX}{K+X}$, where A is the maximum predation rate and K is half saturation constant. The function increase linearly if X is small. At large values of X the slope of the function $F'(X)$ decreases as predator becomes saturated but $F'(X)$ always remains non-negative. Actually, the Holling type-II function is based on the assumption that predation rate is proportional to prey density if prey is scarce. However, if the predator actively seeks out large concentration of prey the Holling type-III function $F(X) = \frac{AX^2}{K^2+X^2}$ is more appropriate. Since the slope of this function goes to zero for small values of X it may be suspected that the food chain will be destabilized if prey concentration becomes too small. The general Holling func-

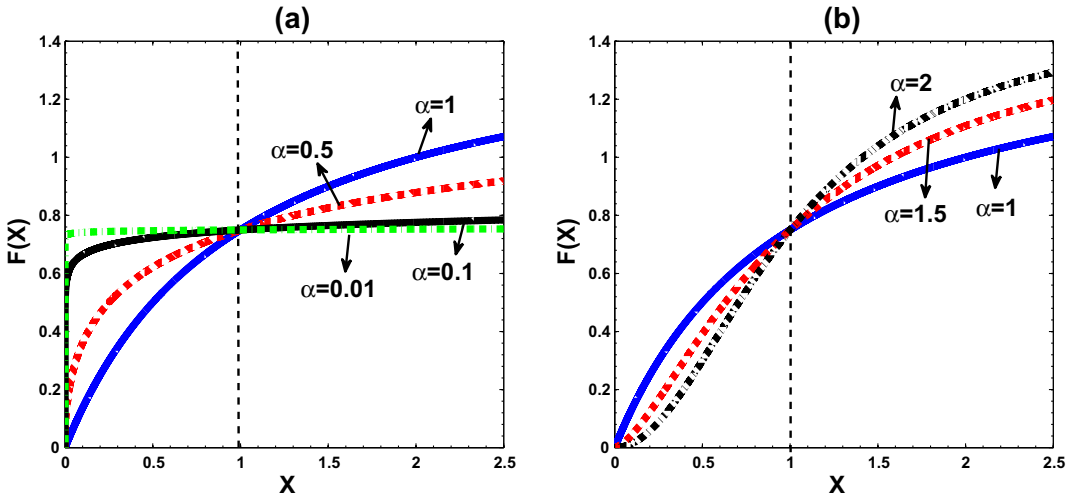

Fig. 1. Comparision of different types of Holling functional responses. (a) For some $\alpha \in (0, 1]$ and (b) for some $\alpha \in [1, 2]$.

tion is defined as $F(X)=\frac{AX^{\alpha}}{K^{\alpha}+X^{\alpha}}$, where $\alpha>0$ ([34–36]). The behaviour of different types response functions are shown in Fig. 1 for different values of α.

We take the following assumptions to formulate the model.

(a) The prey population is divided into two classes, viz. (i) susceptible class whose population density is denoted by S and (ii) infected class whose population density is denoted by I. The intermediate predator whose population density is denoted by P_1 and the density of top-predator is denoted by P_2.
(b) A part of the susceptible prey population becomes infected at a rate γ, following the law of mass action.
(c) Infected population is not in a state of reproduction and also does not compete for the resources.
(d) Behaviour of the entire community is assumed to arise from the coupling of these interacting species, where P_1 preys on both susceptible prey and infected prey in the form of general Holling type and Holling type-I respectively. This different combinations of functional forms are taken because the capturing of infected prey is different from that of susceptible prey. Top-predator preys intermediate predator in the form of general Holling type interaction. This is in contrast to other models which assume particular Holling type interactions ([24–26]).
(e) The infected prey population dies at the rate D_1 and the intermediate predator and top-predator die at the rate D_2 and D_3 respectively.

Under the above assumptions, we obtain the following model:

$$\begin{aligned}
\frac{dS}{dT}&=R_0S\left(1-\frac{S}{K_0}\right)-\gamma IS-C_1A_1\frac{P_1S^{\alpha}}{B_1^{\alpha}+S^{\alpha}}\\
\frac{dI}{dT}&=\gamma IS-A_2P_1I-D_1I\\
\frac{dP_1}{dT}&=A_1\frac{P_1S^{\alpha}}{B_1^{\alpha}+S^{\alpha}}+C_2A_2IP_1-A_3\frac{P_2P_1^{\beta}}{B_2^{\beta}+P_1^{\beta}}-D_2P_1\\
\frac{dP_2}{dT}&=C_3A_3\frac{P_2P_1^{\beta}}{B_2^{\beta}+P_1^{\beta}}-D_3P_2
\end{aligned}\tag{1}$$

Here S,I,P_1,P_2 are respectively the susceptible prey, the infected prey, the intermediate predator and the top-predator population respectively and T is the time. The constant R_0 is the 'intrinsic growth rate' and the constant K_0 is the 'carrying capacity' of species S. A_1 and A_2 are the maximal predation rate of intermediate predator for susceptible and infected prey respectively; A_3 is the maximal predation rate of top-predator for intermediate predator; B_1 and B_2 are the half saturation constant for functional response of intermediate and the top-predator respectively; C_1^{-1} is the conversion rate of susceptible prey to intermediate predator; C_2 is the conversion rate of infected prey to intermediate predator; C_3 is the conversion rate of intermediate predator to top-predator. Here $\alpha(>0)$ and $\beta(>0)$ are the general Holling parameters. From biological point of view, in real world, predators of different species may feed on preys in different types of consumption ways. For example, consider crops, aphids, and lady beetles as prey, intermediate-predator, and top-predator, respectively. In this case, it is natural to assume that the feeding type of aphids on crops is different from that of lady beetles on aphids. Thus, to describe these phenomenon, different types of functional responses are needed.

We nondimensionalize the system (1) with $s=\frac{S}{K_0}$, $i=\frac{I}{K_0}$, $p_1=\frac{P_1}{K_0}$, $p_2=\frac{P_2}{K_0}$, $t=R_0T$ and obtain the following set of equations:

$$\begin{aligned}
\frac{ds}{dt}&=s(1-s)-asi-b\frac{p_1s^{\alpha}}{1+cs^{\alpha}}=F_1(s,i,p_1,p_2),\\
\frac{di}{dt}&=asi-dp_1i-ei=F_2(s,i,p_1,p_2),\\
\frac{dp_1}{dt}&=f\frac{p_1s^{\alpha}}{1+cs^{\alpha}}+gip_1-h\frac{p_2p_1^{\beta}}{1+mp_1^{\beta}}-jp_1=F_3(s,i,p_1,p_2),\\
\frac{dp_2}{dt}&=k\frac{p_2p_1^{\beta}}{1+mp_1^{\beta}}-lp_2=F_4(s,i,p_1,p_2).
\end{aligned}\tag{2}$$

The system (2) has to be analysed with the following initial conditions: $s(0)>0$, $i(0)>0$, $p_1(0)>0$, $p_2(0)>0$; where $a=\frac{\gamma K_0}{R_0}$, $b=\frac{C_1A_1K_0^{\alpha}}{R_0B_1^{\alpha}}$, $c=\frac{K_0^{\alpha}}{B_1^{\alpha}}$, $d=\frac{A_2K_0}{R_0}$, $e=\frac{D_1}{R_0}$, $f=\frac{A_1K_0^{\alpha}}{R_0B_1^{\alpha}}$, $g=\frac{C_2A_2K_0}{R_0}$, $h=\frac{A_3K_0^{\beta}}{R_0B_2^{\beta}}$, $j=\frac{D_2}{R_0}$, $k=\frac{C_3A_3K_0^{\beta}}{R_0B_2^{\beta}}$, $l=\frac{D_3}{R_0}$, $m=\frac{K_0^{\beta}}{B_2^{\beta}}$.

3. Theoretical studies

3.1. Positive invariance

Let $X=(s,i,p_1,p_2)^T\in R^4$ and

$$F(X) = [F_1(X), F_2(X), F_3(X), F_4(X)]^T, \tag{3}$$

where $F(X) : C_+ \to R^4$ and $F \in C_+^\infty(R^4)$. Then system (2) becomes

$$\dot{X} = F(X), \tag{4}$$

with $X(0) = X_0 \in R_+^4$. It is easy to verify that whenever choosing $X(0) \in R^4$ such that $X_i = 0$ then $[F_i(X)]_{X_i=0} \geqslant 0$ (for i = 1,2,3,4). Now any solution of the Eq. (4) with $X_0 \in R_+^4$, say $X(t) = X(t, X_0)$, is such that $X(t) \in R_+^4$ for all $t > 0$ (Nagumo, M. [37]).

3.2. Boundedness

Theorem 1. *All solutions of the system (2) which initiate in R_+^4 are uniformly bounded.*

Proof. Let us consider that $W = s + i + p_1 + p_2$.

Therefore, $\dfrac{dW}{dt} = \dfrac{ds}{dt} + \dfrac{di}{dt} + \dfrac{dp_1}{dt} + \dfrac{dp_2}{dt}$.

Using Eq. (2), we have predator-infected eco-epidemics

$$\frac{dW}{dt} = s(1-s) - (b-f)\frac{p_1 s^\alpha}{1+cs^\alpha} - (d-j)p_1 i - (h-k)\frac{p_2 p_1^\alpha}{1+mp_1^\alpha} - ei - jp_1 - lp_2.$$

since $b \geqslant f, d \geqslant g$ and $h \geqslant k$ we get the following expression:

$$\frac{dW}{dt} \leqslant s(1-s) - ei - jp_1 - lp_2.$$

$$\text{i.e.,} \frac{dW}{dt} \leqslant -(1-s)^2 - (s + i + p_1 + p_2)L + 1,$$

where $L = \min(1, e, j, l)$.

$$\frac{dW}{dt} + LW \leqslant 1 - (1-s)^2.$$

$$\text{This imples } \frac{dW}{dt} + LW \leqslant 1.$$

since $(1-s)^2 \geqslant 0$. Integrating, $We^{Lt} \leqslant \frac{e^{Lt}}{L} + C$, C being arbitrary positive constant. Initially, when $t = 0$, $W = W(s(0),\ i(0),\ p_1(0),\ p_2(0))$. Therefore from the solution, we have $W(s(0),\ i(0),\ p_1(0),\ p_2(0)) \leqslant \frac{1}{L} + C$, i.e., $C \geqslant W(s(0),\ i(0),\ p_1(0),\ p_2(0)) - \frac{1}{L}$.

Therefore,

$We^{Lt} < \frac{e^{Lt}}{L} + W(s(0),\ i(0),\ p_1(0),\ p_2(0)) - \frac{1}{L}$.

Thus, $W < \frac{1-e^{-Lt}}{L} + W(s(0),\ i(0),\ p_1(0),\ p_2(0))e^{-Lt}$.

From the theory of differential inequality we obtain $0 < W < \frac{1-e^{-Lt}}{L} + W(s(0),\ i(0),\ p_1(0),\ p_2(0))e^{-Lt}$.

For $t \to \infty$, we have $0 < W < \frac{1}{L}$.

Hence all the solutions of (2) that initiate in R_+^4 will ultimately remain in the region $B = \{(s, i, p_1, p_2) \in R_+^4 : W = \frac{1}{L} + \eta$, for $\eta > 0\}$. This proves the theorem. □

3.3. Extinction criterion

Lemma 1. *If $1 \leqslant ai(t)$, then $\lim_{t\to\infty} s(t) = 0$. If $as(t) \leqslant e$, then $\lim_{t\to\infty} i(t) = 0$. If $f \leqslant cj$ and $gi(t) \leqslant j$, then $\lim_{t\to\infty} p_1(t) = 0$. If $k \leqslant ml$, then $\lim_{t\to\infty} p_2(t) = 0$.*

Proof. We have

$$\frac{ds}{dt} = s(1-s) - asi - b\frac{p_1 s^\alpha}{1+cs^\alpha} \leqslant s(1-ai).$$

Solving above equation we have $s(t) \leqslant s(t_0)exp\left(\int_{t_0}^t (1-ai(r))dr\right)$. Hence $\lim_{t\to\infty} s(t) = 0$, provided $1 \leqslant ai(t)$.

Now

$$\frac{di}{dt} = asi - dp_1 i - ei.$$

Therefore, $i(t) = i(t_0)exp\left(\int_{t_0}^{t}(as(r) - dp_1(r) - e)dr\right)$.

$i(t) \leqslant i(t_0)exp\left(\int_{t_0}^{t}(as(r) - e)dr\right)$.

Thus, $\lim_{t\to\infty} i(t) = 0$, provided $as(t) \leqslant e$.

$$\frac{dp_1}{dt} = f\frac{p_1 s^\alpha}{1+cs^\alpha} + gip_1 - h\frac{p_2 p_1^\beta}{1+mp_1^\beta} - jp_1.$$

Therefore,

$$\frac{dp_1}{dt} \leqslant f\frac{p_1 s^\alpha}{1+cs^\alpha} + gip_1 - jp_1.$$

Therefore, $p_1(t) \leqslant p_1(t_0)exp\left(\int_{t_0}^{t}\left(\frac{fs^\alpha(r)}{1+cs^\alpha(r)} + gi(r) - j\right)dr\right)$,

i.e, $p_1(t) \leqslant p_1(t_0)exp\left(\int_{t_0}^{t}\left((f-cj)\frac{s^\alpha(r)}{1+cs^\alpha(r)} + gi(r) - j\right)dr\right)$.

Thus, if $f \leqslant cj$ and $gi(t) \leqslant j$, then $\lim_{t\to\infty} p_1(t) = 0$.

Now,

$$\frac{dp_2}{dt} = k\frac{p_2 p_1^\beta}{1+mp_1^\beta} - lp_2.$$

$p_2(t) = p_2(t_0)exp\left(\int_{t_0}^{t}\left(\frac{kp_1^\beta(r)}{1+mp_1^\beta(r)} - l\right)dr\right)$,

i.e., $p_2(t) \leqslant p_2(t_0)exp(-l(t-t_0))$.

Thus, $\lim_{t\to\infty} p_2(t) = 0$, provided $k \leqslant ml$. □

4. Existence and local stability of equilibrium points

The system has seven equilibrium points. $E_0(0,0,0,0)$ is the trivial equilibrium point. The axial equilibrium point is $E_1(1,0,0,0)$. Disease free planar equilibrium point is $E_2(\theta_1, 0, \theta_2, 0)$, where $\theta_1^\alpha = \frac{j}{f-cj}, \theta_2 = \frac{f(1-\theta_1)}{b\theta_1 j}$.

The existence condition of disease free planer equilibrium point E_2 are $f - cj > 0$ and $1 > \theta_1$.

The endemic planar equilibrium point is $E_3\left(\frac{e}{a},\ \frac{(a-e)}{a^2},\ 0,\ 0\right)$. where $a - e > 0$. $E_4(\bar{s},\ 0,\ \bar{p_1},\ \bar{p_2})$ is disease free space equilibrium point where

$\bar{p_1}^\beta = \frac{l}{k-ml},\ \bar{p_2} = \frac{k\{f\bar{s}^\alpha - j(c\bar{s}^\alpha+1)j\}}{h(1+c\bar{s}^\alpha)lp_1}$ and $\bar{s}$ are the positive roots of the equation $c\bar{s}^{\alpha+1} + c\bar{s}^\alpha - \bar{p_1}b\bar{s}^{\alpha-1} - \bar{s} + 1 = 0$. The disease free equilibrium point E_4 exists if $k > ml, f\bar{s}^\alpha > j(1 + c\bar{s}^\alpha)$.

$E_5(\hat{s},\ \hat{i},\ \hat{p_1}, 0)$ is the top-predator free equilibrium point where $\hat{s} = \frac{e+d\hat{p_1}}{a}$,

$\hat{i} = \frac{j}{g} - \frac{f(e+d\hat{p_1})^\alpha}{g[a^\alpha+c(e+d\hat{p_1})^\alpha]}$ and $\hat{p_1}$ are the positive roots of the equation

$gcd\hat{p_1}(e+d\hat{p_1})^\alpha + (acg - a^2cj - fa)(e+d\hat{p_1})^\alpha - ba^2g\hat{p_1}(e+d\hat{p_1})^{\alpha-1} - a^\alpha g(e+d\hat{p_1}) + ga^{\alpha+1} - ja^{\alpha+2} = 0$,

The top-predator free equilibrium point E_5 exists if $j > \frac{ef+df\hat{p_1}^\beta}{a+ce+cd\hat{p_1}^\beta}$.

The interior equilibrium point is given by $E^*(s^*,\ i^*,\ p_1^*,\ p_2^*)$, where $s^* = \frac{dp_1^*+e}{a}$. $i^* = \frac{1-s^*}{a} - \frac{bp_1^* s^{*\alpha-1}}{a(1+cs^{*\alpha})}$. $p_1^{*\beta} = \frac{l}{k-ml}$ and $p_2^* = \frac{1+mp_1^{*\beta}}{p_1^{*\beta-1}h}\left[\frac{fs^{*\alpha}}{1+cs^{*\alpha}} + gi - j\right]$.

The interior equilibrium point E^* exists if $1 > s^* + \frac{bp_1^* s^{*\alpha-1}}{1+cs^{*\alpha}}$, $k > ml$, $\frac{fs^{*\alpha}}{1+cs^{*\alpha}} + gi^* > j$.

The Jacobian matrix J of the system (2) at an arbitrary point (s,i,p_1,p_2) is given by

$$J = \begin{pmatrix} F_{1s} & F_{1i} & F_{1p_1} & 0 \\ F_{2s} & F_{2i} & F_{2p_1} & 0 \\ F_{3s} & F_{3i} & F_{3p_1} & F_{3p_2} \\ 0 & 0 & F_{4p_1} & F_{4p_2} \end{pmatrix}. \tag{5}$$

Theorem 2. *The trivial equilibrium point E_0 is always unstable. The disease free planar equilibrium point E_2 is locally stable if $\frac{k\theta_2^\beta}{1+m\theta_2^\beta} < l, a\theta_1 < d\theta_2 + e, \frac{b\theta_2\theta_1^{\alpha-1}[(1+c\theta_1^\alpha)-\alpha]}{(1+c\theta_1^\alpha)^2} < \theta_1$. The endemic planar equilibrium point E_3 is locally stable if $\frac{fe^\alpha}{a^\alpha+ce^\alpha} + \frac{g(a-e)}{a^2} < j$.*

Proof. Since an eigenvalue associated with the Jacobian matrix at E_0 is 1, so E_0 is an unstable equilibrium point.

The Jacobian matrix J_1 at E_1 is given by

$$J_1 = \begin{pmatrix} -1 & -a & -\frac{b}{1+c} & 0 \\ 0 & a-e & 0 & 0 \\ 0 & 0 & \frac{f}{1+c}-j & 0 \\ 0 & 0 & 0 & -l \end{pmatrix}.$$

From the Jacobian matrix J_1, it is observed that equilibrium point E_1 is unstable if $a > e$ and $f > (c+1)j$, which are the existence condition for the equilibrium points E_2 and E_3.

The Jacobian matrix J_2 at E_2 is given by

$$J_2 = \begin{pmatrix} \frac{b\theta_2\theta_1^{\alpha-1}[(1+c\theta_1^{\alpha})-\alpha]}{(1+c\theta_1^{\alpha})^2} - \theta_1 & -a\theta_1 & -\frac{b\theta_1^{\alpha}}{1+c\theta_1^{\alpha}} & 0 \\ 0 & a\theta_1 - d\theta_2 - e & 0 & 0 \\ \frac{f\theta_2\alpha\theta_1^{(\alpha-1)}}{(1+c\theta_1^{\alpha})^2} & g\theta_2 & 0 & -\frac{h\theta_2^{\beta}}{1+m\theta_2^{\beta}} \\ 0 & 0 & 0 & \frac{k\theta_2^{\beta}}{1+m\theta_2^{\beta}} - l \end{pmatrix}.$$

The characteristic roots of J_2 are $a\theta_1 - d\theta_2 - e$ and $\frac{k\theta_2^{\beta}}{1+m\theta_2^{\beta}} - l$ and the roots of the equation $\lambda^2 - \left[\frac{b\theta_2\theta_1^{\alpha-1}[(1+c\theta_1^{\alpha})-\alpha]}{(1+c\theta_1^{\alpha})^2} - \theta_1\right]\lambda + \frac{bf\theta_2\alpha\theta_1^{(2\alpha-1)}}{(1+c\theta_1^{\alpha})^3} = 0$.

Hence, E_2 is stable if the conditions given in the theorem are satisfied

The Jacobian matrix J_3 at E_3 is given by

$$J_3 = \begin{pmatrix} -\frac{e}{a} & -e & -\frac{be^{\alpha}}{a^{\alpha}+ce^{\alpha}} & 0 \\ \frac{a-e}{a} & 0 & -\frac{d(a-e)}{a^2} & 0 \\ 0 & 0 & \frac{fe^{\alpha}}{a^{\alpha}+ce^{\alpha}} + \frac{g(a-e)}{a^2} - j & 0 \\ 0 & 0 & 0 & -l \end{pmatrix}.$$

The characteristic roots of J_3 are $-l$, $\frac{fe^{\alpha}}{a^{\alpha}+ce^{\alpha}} + \frac{g(a-e)}{a^2} - j$ and the roots of the equation $\lambda^2 + \frac{e}{a}\lambda + \frac{e(a-e)}{a} = 0$. □

Hence, the equilibrium point E_3 is stable if $\frac{fe^{\alpha}}{a^{\alpha}+ce^{\alpha}} + \frac{g(a-e)}{a^2} < j$.

Theorem 3. *The disease free equilibrium point E_4 is locally stable if*

$$\frac{\bar{p_1}b\bar{s}^{\alpha-1}[(1+c\bar{s}^{\alpha})-\alpha]}{(1+c\bar{s}^{\alpha})^2} < \bar{s}, \quad a\bar{s} < d\bar{p_1} + e, \quad (1+m\bar{p_1}^{\beta}) < \beta \tag{6}$$

and the top-predator free equilibrium point E_5 is stable if

$$\frac{k\hat{p_1}^{\beta}}{1+m\hat{p_1}^{\beta}} < l, \quad \frac{\hat{p_1}b\hat{s}^{\alpha-1}[(1+c\hat{s}^{\alpha})-\alpha]}{(1+c\hat{s}^{\alpha})^2} < \hat{s}, \quad fd\alpha\hat{s}^{(\alpha-1)} \leqslant (1+c\hat{s}^{\alpha})bg. \tag{7}$$

Proof. The Jacobian matrix J_4 at E_4 is given by

$$J_4 = \begin{pmatrix} \frac{\bar{p_1}b\bar{s}^{\alpha-1}[(1+c\bar{s}^{\alpha})-\alpha]}{(1+c\bar{s}^{\alpha})^2} - \bar{s} & -a\bar{s} & -\frac{b\bar{s}^{\alpha}}{1+c\bar{s}^{\alpha}} & 0 \\ 0 & a\bar{s} - d\bar{p_1} - e & 0 & 0 \\ \frac{f\alpha\bar{p_1}\bar{s}^{(\alpha-1)}}{(1+c\bar{s}^{\alpha})^2} & g\bar{p_1} & \frac{\bar{p_2}h\bar{p_1}^{\beta-1}[(1+m\bar{p_1}^{\beta})-\beta]}{(1+m\bar{p_1}^{\beta})^2} & -\frac{h\bar{p_1}^{\beta}}{1+m\bar{p_1}^{\beta}} \\ 0 & 0 & \frac{k\beta\bar{p_2}\bar{p_1}^{(\beta-1)}}{(1+m\bar{p_1}^{\beta})^2} & 0 \end{pmatrix}.$$

The characteristic roots of the Jacobian matrix J_4 are $a\bar{s} - d\bar{p_1} - e$, and the roots of the characteristic equation is given by $\lambda^3 + \Omega_1\lambda^2 + \Omega_2\lambda + \Omega_3 = 0$. where

$$\Omega_1 = -\left[\left(\frac{\bar{p_1}b\bar{s}^{\alpha-1}[(1+c\bar{s}^{\alpha})-\alpha]}{(1+c\bar{s}^{\alpha})^2} - \bar{s}\right) + \left(\frac{\bar{p_2}h\bar{p_1}^{\beta-1}[(1+m\bar{p_1}^{\beta})-\beta]}{(1+m\bar{p_1}^{\beta})^2}\right)\right],$$

$$\Omega_2 = \frac{hk\beta\bar{p_2}\bar{p_1}^{(2\beta-1)}}{(1+m\bar{p_1}^{\beta})^3} + \left[\frac{\bar{p_2}h\bar{p_1}^{\beta-1}[(1+m\bar{p_1}^{\beta})-\beta]}{(1+m\bar{p_1}^{\beta})^2}\right]\left[\frac{\bar{p_1}b\bar{s}^{\alpha-1}[(1+c\bar{s}^{\alpha})-\alpha]}{(1+c\bar{s}^{\alpha})^2} - \bar{s}\right] + \frac{bf\bar{p_1}\alpha\bar{s}^{(2\alpha-1)}}{(1+c\bar{s}^{\alpha})^3},$$

$$\Omega_3 = -\left[\frac{\bar{p_1}b\bar{s}^{\alpha-1}[(1+c\bar{s}^{\alpha})-\alpha]}{(1+c\bar{s}^{\alpha})^2} - \bar{s}\right]\frac{kh\beta\bar{p_2}\bar{p_1}^{(2\beta-1)}}{(1+m\bar{p_1}^{\beta})^3}.$$

Hence, by Routh–Hurwitz criterion [38] the equilibrium point E_4 is stable if the condition 6 holds.

The Jacobian matrix J_5 at E_5 is given by

$$J_5 = \begin{pmatrix} \frac{\hat{p_1} b\hat{s}^{\alpha-1}[(1+c\hat{s}^{\alpha})-\alpha]}{(1+c\hat{s}^{\alpha})^2} - \hat{s} & -a\hat{s} & -\frac{b\hat{s}^{\alpha}}{1+c\hat{s}^{\alpha}} & 0 \\ a\hat{i} & 0 & -d\hat{i} & 0 \\ \frac{f\alpha\hat{p_1}\hat{s}^{(\alpha-1)}}{(1+c\hat{s}^{\alpha})^2} & g\hat{p_1} & 0 & -\frac{h\hat{p_1}^{\beta}}{1+m\hat{p_1}^{\beta}} \\ 0 & 0 & 0 & \frac{k\hat{p_1}^{\beta}}{1+m\hat{p_1}^{\beta}} - l \end{pmatrix}.$$

The characteristic roots of the Jacobian matrix J_5 are $\frac{k\hat{p_1}^{\beta}}{1+m\hat{p_1}^{\beta}} - l$, and the roots of the equation is given by $\lambda^3 + \Theta_1\lambda^2 + \Theta_2\lambda + \Theta_3 = 0$. where

$$\Theta_1 = -\left[\frac{\hat{p_1} b\hat{s}^{\alpha-1}[(1+c\hat{s}^{\alpha})-\alpha]}{(1+c\hat{s}^{\alpha})^2} - \hat{s}\right],$$

$$\Theta_2 = \left[d\hat{i}g\hat{p_1} + \frac{bf\hat{p_1}\alpha\hat{s}^{(2\alpha-1)}}{(1+c\hat{s}^{\alpha})^3} + a^2\hat{s}\hat{i}\right],$$

$$\Theta_3 = -\left[\left(\frac{\hat{p_1} b\hat{s}^{\alpha-1}[(1+c\hat{s}^{\alpha})-\alpha]}{(1+c\hat{s}^{\alpha})^2} - \hat{s}\right)(d\hat{i}g\hat{p_1}) - \frac{af\alpha d\hat{p_1}\hat{i}\hat{s}^{(2\alpha-1)}}{(1+c\hat{s}^{\alpha})^2} + \left(-\frac{b\hat{s}^{\alpha}}{1+c\hat{s}^{\alpha}}\right)(a\hat{i}g\hat{p_1})\right].$$

Hence, by Routh–Hurwitz criterion [38] the equilibrium point E_5 is stable if the conditions 7 hold. □

Theorem 4. *The interior equilibrium point $E^*(s^*, i^*, p_1^*, p_2^*)$ for the system (2) is locally asymptotically stable if the following conditions hold as follows:*

$\sigma_1 > 0$, $\sigma_1\sigma_2 - \sigma_3 > 0$, $\sigma_3(\sigma_1\sigma_2 - \sigma_3) - \sigma_4\sigma_1^2 > 0$, *where σ_i's are given in the proof of the theorem.*

Proof. The Jacobian matrix at the interior point $E^*(s^*, i^*, p_1^*, p_2^*)$ is

$$V = \begin{pmatrix} A_{11} & A_{12} & A_{13} & A_{14} \\ A_{21} & A_{22} & A_{23} & A_{24} \\ A_{31} & A_{32} & A_{33} & A_{34} \\ A_{41} & A_{42} & A_{43} & A_{44} \end{pmatrix}.$$

Where

$$A_{11} = \frac{p_1^* b{s^*}^{\alpha-1}[(1+cs^{*\alpha})-\alpha]}{(1+cs^{*\alpha})^2} - s^*,\ A_{12} = -as^*,\ A_{13} = -\frac{b{s^*}^{\alpha}}{1+cs^{*\alpha}},\ A_{14} = 0, A_{21} = ai^*,\ A_{22} = 0,\ A_{23} = -di^*,\ A_{24} = 0,\ A_{31} = \frac{f\alpha p_1^* {s^*}^{(\alpha-1)}}{(1+cs^{*\alpha})^2},\ A_{32} = gp_1^*,\ A_{33} = \frac{p_2^* h{p_1^*}^{\beta-1}[(1+mp_1^{*\beta})-\beta]}{(1+mp_1^{*\beta})^2},\ A_{34} = -\frac{hp_1^{*\beta}}{1+mp_1^{*\beta}},\ A_{41} = 0,\ A_{42} = 0,\ A_{43} = \frac{k\beta p_2^* {p_1^*}^{(\beta-1)}}{(1+mp_1^{*\beta})^2},\ A_{44} = 0$$

.

The characteristic equation of Jacobian matrix V is given by

$\lambda^4 + \sigma_1\lambda^3 + \sigma_2\lambda^2 + \sigma_3\lambda + \sigma_4 = 0$. where

$$\sigma_1 = -[A_{11} + A_{22} + A_{33} + A_{44}],$$

$$\sigma_2 = -A_{34}A_{43} + A_{11}A_{33} - A_{32}A_{23} - A_{21}A_{12} + A_{13}A_{31},$$

$$\sigma_3 = (A_{34}A_{43} + A_{32}A_{23})A_{11} + A_{21}A_{12}A_{33} + A_{12}A_{23}A_{31} + A_{32}A_{21}A_{13},$$

$$\sigma_4 = A_{12}A_{21}A_{34}A_{43}.$$

Using the Routh–Hurwitz criteria [38] we observe that the system (2) is stable around the positive equilibrium point E^* if the conditions stated in the theorem hold. □

5. Permanence and impermanence of the system

From biological point of view, permanence of a system means the survival of all species of the system in future time. Mathematically, permanence of a system means that strictly positive solutions do not have omega (Ω) limit points on the boundary of the non-negative cone.

Theorem 5. *Let $f > (c+1)j$ and $a > e$ and the following conditions are satisfied*

(i) $\frac{fe^{\alpha}}{a^{\alpha}+ce^{\alpha}} + \frac{g(a-e)}{a^2} > j$,
(ii) $a\bar{s} > e + d\bar{p_1}$,
(iii) $\frac{k\bar{p_1}^{\beta}}{(1+m\bar{p_1}^{\beta})} > l$.

Further if there exists finite number of periodic solutions $s = \phi_r(t),\ p_1 = \psi_r(t),\ r = 1,2,3,\ldots\ldots..,n$ in the $s-p_1$ plane, then system (2) is uniformly persistent provided for each periodic solutions of period T.

$\eta_r = -e + \frac{1}{T}\int_0^T (a\phi_r - d\psi_r)dt > 0, \quad r = 1,2,\ldots\ldots..,n.$

Proof. Let χ be a point in the positive quadrant and $o(\chi)$ be orbit through χ and Ω be the omega limit set of the orbit through χ. Note that $\Omega(\chi)$ is bounded.

We claim that $E_0 \notin \Omega(\chi)$. If $E_0 \in \Omega(\chi)$ then by the Butler–McGehee lemma there exist a point P in $\Omega \bigcap W^s(E_0)$ where $W^s(E_0)$ denotes the stable manifold of E_0. Since $O(p)$ lies in $\Omega(\chi)$ and $W^s(E_0)$ is the $i-p_1-p_2$ space, we conclude that $o(P)$ is unbounded, which is a contradiction.

Next $E_1 \notin \Omega(\chi)$, for otherwise, since E_1 is a saddle point (which follows from the existence of E_2 and E_3) by the Butler–McGehee lemma there exist a point P in $\Omega \bigcap W^s(E_1)$. Now $W^s(E_1)$ is the $s-p_2$ plane implies that an unbounded orbit lies in $\Omega(\chi)$, a contradiction.

Next we show that $E_3 \notin \Omega(\chi)$. If $E_3 \in \Omega(\chi)$, the condition $\frac{fe^{\alpha}}{a^{\alpha}+ce^{\alpha}} + \frac{g(a-e)}{a^2} > j$ implies that E_3 is saddle point. $W^s(E_3)$ is the $s-i-p_2$ space and hence the orbits in this space emanate either E_0 or E_1 or an unbounded lies in $\Omega(\chi)$, again a contradiction.

The condition $a\bar{s} > d\bar{p_1} + e$ implies that E_4 is a unstable point and also the contradiction, $\frac{k\bar{p_1}^{\beta}}{(1+m\bar{p_1}^{\beta})} > l$ implies that E_5 is unstable. So by similar arguments we can show that $E_4 \notin \Omega(\chi)$ and $E_5 \notin \Omega(\chi)$.

Lastly we show that no periodic orbits in the $s-p_1$ or $E_2 \in \Omega(\chi)$. Let $r_i,\ i = 1,2,\ldots\ldots..,n$ denote the closed orbit of the periodic solution $(\phi_r(t), \psi_r(t))$ in $s-p_1$ plane such that r_i lies inside $r_{(i-1)}$. Let the Jacobian matrix J given in (6) corresponding to r_i is denoted by $J_r(\phi_r(t), 0, \psi_r(t), 0)$. □

Computing the fundamental matrix of linear periodic system, $X' = J_r(t)X,\ X(0) = X_0$.

We find that its Floquet multiplier in the i direction is $e^{(\eta_1 T)}$. Then proceeding in an analogous manner like Kumar and Freedman [39], we conclude that no r_i lies on $\Omega(\chi)$. Thus, $\Omega(\chi)$ lines in the positive quadrant and system (2) is persistent. Finally, since only the closed orbits and the equilibria from the omega limit set of the solutions on boundary of R^4 and system (2) is dissipative. Now using a theorem of Butler et al. [40], we conclude that system (2) is uniformly persistent.

Theorem 6. *Let $f > (c+1)j$ and $a > e$ and the following conditions are satisfied*

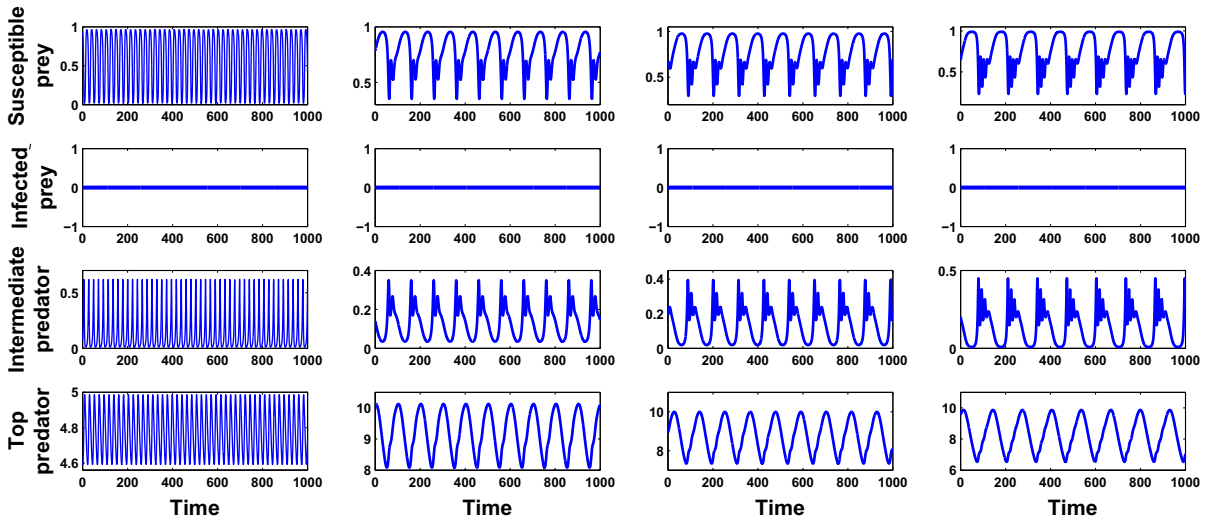

Fig. 2. Plots of Susceptible prey, Infected prey, Intermediate predator, Top-predator vs. time in the system (2) for different values of α, β and a.

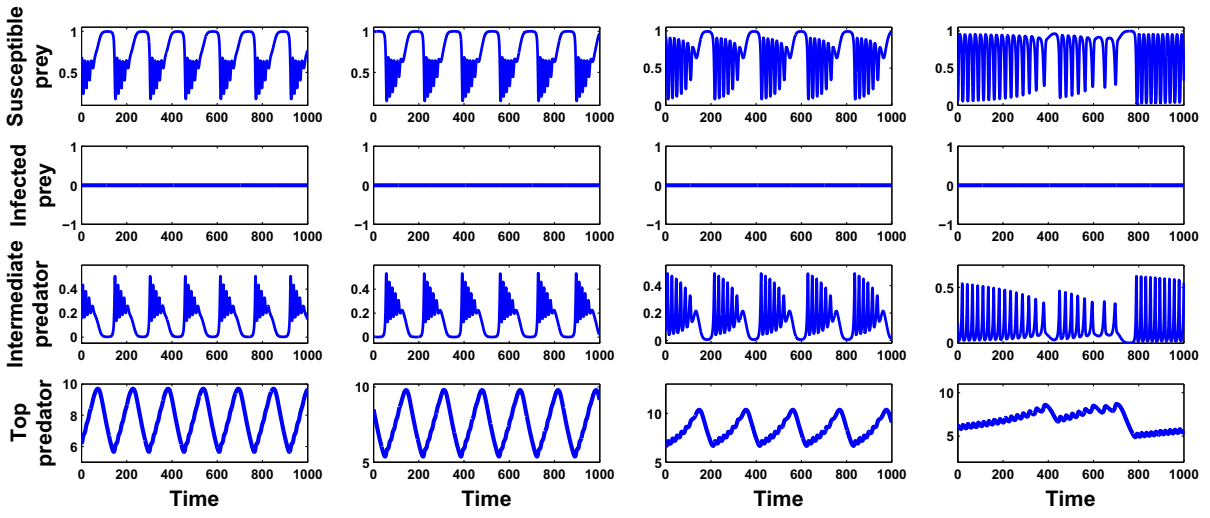

Fig. 3. Plots of Susceptible prey, Infected prey, Intermediate predator, Top-predator vs. time in the system (2) for different values of α, β and a.

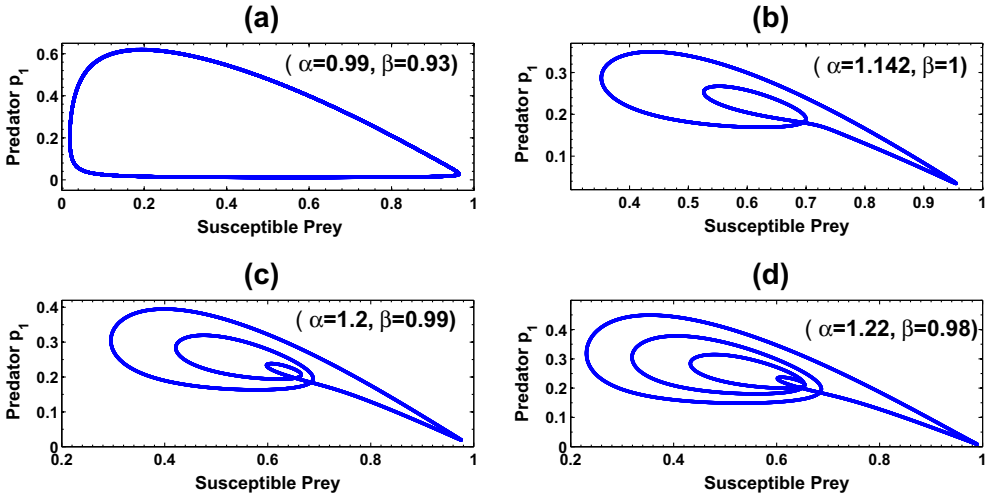

Fig. 4. Figure depicts the Limit Cycle, Period-2, Period-3 and Period-4 behaviour of the system (2) for different values of α and β with infection rate $a = 1.15$.

(i) $\frac{fe^{\alpha}}{a^{\alpha}+ce^{\alpha}} + \frac{g(a-e)}{a^2} > j$,
(ii) $a\bar{s}^{\alpha} > e + d\bar{p_1}$,
(iii) $min\{\frac{k\bar{p_1}^{\beta}}{(1+m\bar{p_1}^{\beta})}, \frac{k\theta_2^{\beta}}{1+m\theta_2^{\beta}}\} > l$.

and there exists no limit cycle in the $s - p_1$ plane, the system (2) is uniformly persistent.

Proof. Proof of the Theorem (6) is obvious and so omitted.

Before obtaining condition for impermanence of system (2), we briefly define the impermanence of a system. Let $\chi = (\chi_1, \chi_2, \chi_3, \chi_4)$ be the population, vector, let $E = \{\chi : \chi_1, \chi_2, \chi_3, \chi_4 > 0\}$, and ∂D is the boundary of D. $\rho(\ldots)$ is the distance in R_+^4.

Let us consider the system of equation is

$$\dot{\chi} = \chi_i f_1(\chi), \quad i = 1, 2, 3, 4$$

where $f_i : R_+^4 \to R$ and $f_i \in C^1$.

The semi orbit γ^+ is defined by the set $\{\chi(t) : t > 0\}$ where $\chi(t)$ is the solution with initial value $\chi(0) = \chi_0$.

The above system is said to be impermanent [41] if and only if there is an $\chi \in D$ such that $\lim_{t\to\infty} \rho(\chi(t), \partial D) = 0$. Thus a community is impermanent if there is at least one semi orbit which tends to boundary. □

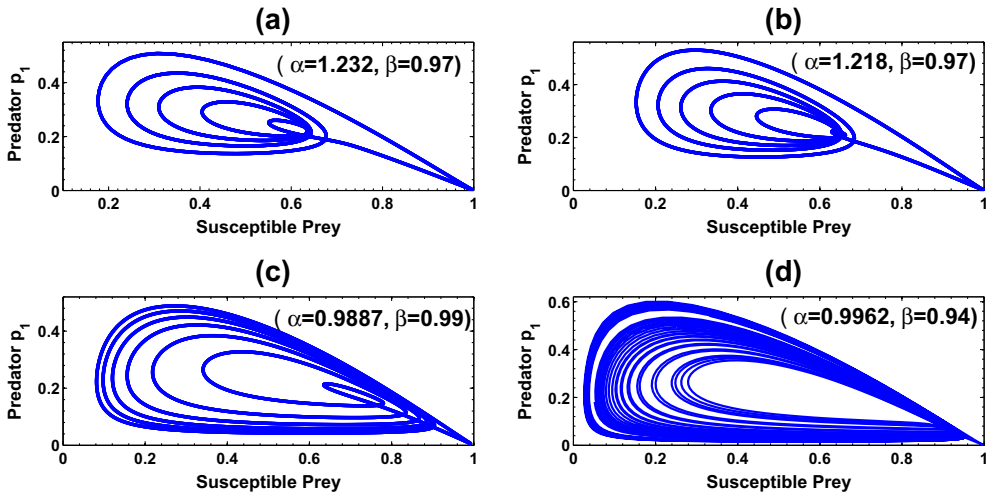

Fig. 5. Figure depicts the Period-5, Period-6, Period-7 and Chaotic behaviour of the system (2) for different values of α and β with infection rate $a = 1.15$.

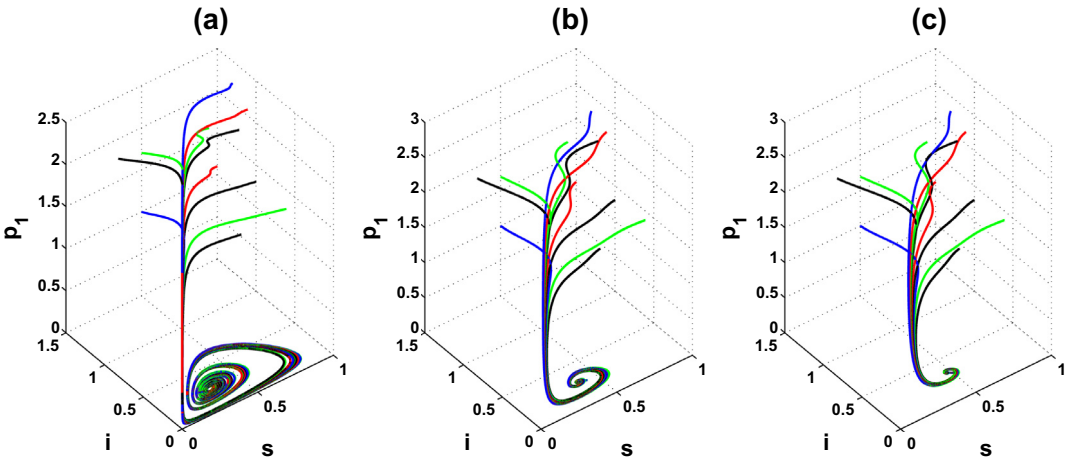

Fig. 6. Global stability of the system (2) with different initial conditions for (a)$\alpha = 1.2, \beta = 0.98$, (b) $\alpha = 1.5, \beta = 0.98$, (c) $\alpha = 1.8, \beta = 0.98$.

Theorem 7. *Let $f > (c+1)j$ and $a > e$ and if the condition $\frac{fe^{\alpha}}{a^{\alpha}+ce^{\alpha}} + \frac{g(a-e)}{a^2} < j$ holds, then the system (2) is impermanent.*

Proof. The conditions $f > (c+1)j$ and $a > e$ are obtain from existence of the equilibria points E_2 and E_3. The given condition $\frac{fe^{\alpha}}{a^{\alpha}+ce^{\alpha}} + \frac{g(a-e)}{a^2} < j$ implies that E_3 is a saturated equilibrium point on boundary. Hence, there exist at least one orbit in the interior that converges to the boundary (Hofbauer, [42]).

Consequently the system (2) is impermanent (Hutson and Law, [41]). □

6. Global stability

We have determined the conditions for global stability of interior equilibrium point through the following theorem.

Theorem 8. *The sufficient conditions for the system (2) is to be globally asymptotically stable around the equilibrium $E^*(s^*,\ i^*,\ p_1^*,\ p_2^*)$ if $d > g,\ b > f,\ h > k$ and $\mu = \left[bp_1\left(\frac{s^*s^{\alpha-1}}{1+cs^{\alpha}} + \frac{ss^{*\alpha-1}}{1+cs^{*\alpha}}\right) + f\left(\frac{s^{*\alpha}p_1^*}{1+cs^{*\alpha}} - \frac{s^{\alpha}p_1^*}{1+cs^{\alpha}}\right) + hp_2\left(\frac{p_1^*p_1^{\beta-1}}{1+mp_1^{\beta}} + \frac{p_1p_1^{*\beta-1}}{1+mp_1^{*\beta}}\right) + k\left(\frac{p_1^{\beta}p_2^*}{1+mp_1^{*\beta}} - \frac{p_1^{\beta}p_2^*}{1+mp_1^{\beta}}\right)\right] < 0.$*

Proof. We first choose a Lyapunov function defined as follows:

$$V(s,i,p_1,p_2) = \int_{s^*}^{s} \frac{s-s^*}{s}ds + \int_{i^*}^{i} \frac{i-i^*}{i}di + \int_{p_1^*}^{p_1} \frac{p_1-p_1^*}{p_1}dp_1 + \int_{p_2^*}^{p_2} \frac{p_2-p_2^*}{p_2}dp_2. \tag{8}$$

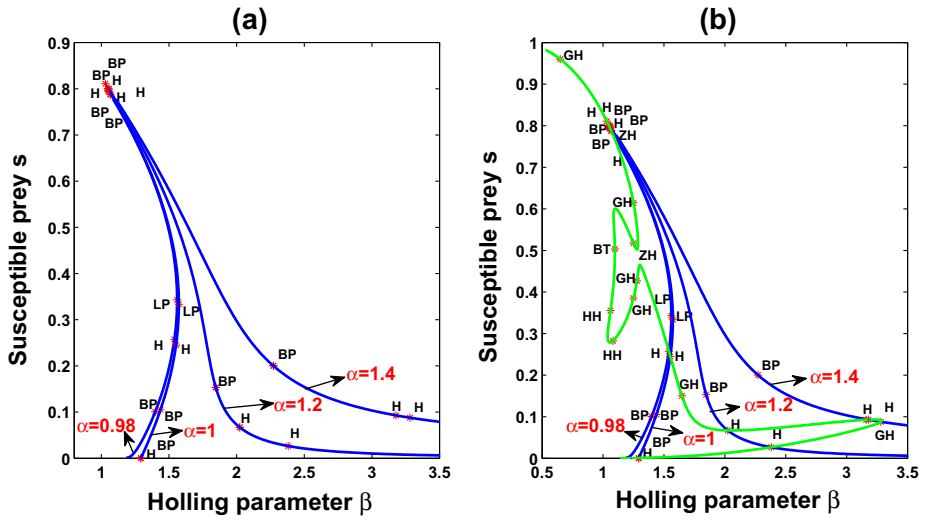

Fig. 7. Figure depicts (a) Continuation curves of equilibrium with the variation of the parameter β of the variable s. (b) Hopf point continuation of the system: GH-generalized Hopf; BT-Bogdanov Takens; ZH-zero Hopf point, HH-Neutral saddle.

Calculating time derivative of the Eq. (8) along the solutions of the system (2) gives us

$$\begin{aligned}
\frac{dV}{dt} &= \frac{(s-s^*)}{s}\frac{ds}{dt} + \frac{(i-i^*)}{i}\frac{di}{dt} + \frac{(p_1-p_1^*)}{p_1}\frac{dp_1}{dt} + \frac{(p_2-p_2^*)}{p_2}\frac{dp_2}{dt} \\
&= (s-s^*)\left\{-(s-s^*) - a(i-i^*) - bp_1\left(\frac{s^{\alpha-1}}{1+cs^\alpha} - \frac{s^{*\alpha-1}}{1+cs^{*\alpha}}\right)\right\} \\
&\quad + (i-i^*)\{a(s-s^*) - d(p_1-p_1^*)\} + (p_1-p_1^*)\left\{f\left(\frac{s^\alpha}{1+cs^\alpha} - \frac{s^{*\alpha}}{1+cs^{*\alpha}}\right) + g(i-i^*) - hp_2\left(\frac{p_1^{\beta-1}}{1+mp_1^\beta} - \frac{p_1^{*\beta-1}}{1+mp_1^{*\beta}}\right)\right\} \\
&\quad + (p_2-p_2^*)\left\{k\left(\frac{p_1^\beta}{1+mp_1^\beta} - \frac{p_1^{*\beta}}{1+mp_1^{*\beta}}\right)\right\}. = -(s-s^*)^2 - (d-g)(i-i^*)(p_1-p_1^*) - (b-f)\frac{p_1 s^\alpha}{1+cs^\alpha} - (b+f)\frac{p_1 s^{*\alpha}}{1+cs^{*\alpha}} \\
&\quad + bp_1\left(\frac{s^* s^{\alpha-1}}{1+cs^\alpha} + \frac{ss^{*\alpha-1}}{1+cs^{*\alpha}}\right) + f\left(\frac{s^{*\alpha}p_1^*}{1+cs^{*\alpha}} - \frac{s^\alpha p_1^*}{1+cs^\alpha}\right) - (h-k)\frac{p_2 p_1^\beta}{1+mp_1^\beta} - (h+k)\frac{p_2 p_1^{*\beta}}{1+mp_1^{*\beta}} \\
&\quad + hp_2\left(\frac{p_1^* p_1^{\beta-1}}{1+mp_1^\beta} + \frac{p_1 p_1^{*\beta-1}}{1+mp_1^{*\beta}}\right) + k\left(\frac{p_1^{*\beta}p_2^*}{1+mp_1^{*\beta}} - \frac{p_1^\beta p_2^*}{1+mp_1^\beta}\right).
\end{aligned}$$

Thus, $\frac{dV}{dt} < 0$, provided $d > g, b > f, h > k$ and $\mu = \left[bp_1\left(\frac{s^* s^{\alpha-1}}{1+cs^\alpha} + \frac{ss^{*\alpha-1}}{1+cs^{*\alpha}}\right) + f\left(\frac{s^{*\alpha}p_1^*}{1+cs^{*\alpha}} - \frac{s^\alpha p_1^*}{1+cs^\alpha}\right) + hp_2\left(\frac{p_1^* p_1^{\beta-1}}{1+mp_1^\beta} + \frac{p_1 p_1^{*\beta-1}}{1+mp_1^{*\beta}}\right) + k\left(\frac{p_1^{*\beta}p_2^*}{1+mp_1^{*\beta}} - \frac{p_1^\beta p_2^*}{1+mp_1^\beta}\right)\right] < 0.$

Hence the theorem folllows. □

7. Results

We illustrate some of the key findings using numerical simulations. We assume the parameter values $b = 5,\ d = 3,\ e = 0.5,\ f = 5,\ g = 2.5,\ h = 0.1,\ m = 2,\ j = 0.4,\ k = 0.1,\ l = 0.01,\ c = 3,$ which remain unchanged for all numerical simulations. The main goal of this paper is to investigate the effects of infection rate a as well as the effects of different types of interactions for different values of α and β.

For $a = 1.6$ and $\alpha = 1.36,\ \beta = 0.98$ we obtain the positive interior equilibrium point $E^*(0.5371, 0.1585, 0.1198, 11.1964)$. For the above set of parameter values we have $\sigma_1 = 0.2504 > 0,\ \sigma_4 = 0.0016 > 0,\ \sigma_1\sigma_2 - \sigma_3 = 0.0367 > 0$ and $\sigma_3(\sigma_1\sigma_2 - \sigma_3) - \sigma_4\sigma_1^2 = 0.0000203 > 0$ which implies that the system (2) is locally asymptotically stable around positive equilibrium E^*.

We have shown system's dynamics for different values of α, β and infection rate a in Fig. 2 and Fig. 3. From Fig. 2 and Fig. 3, we observe that the system (2) have periodic oscillations as well as chaotic bands for different general Holling

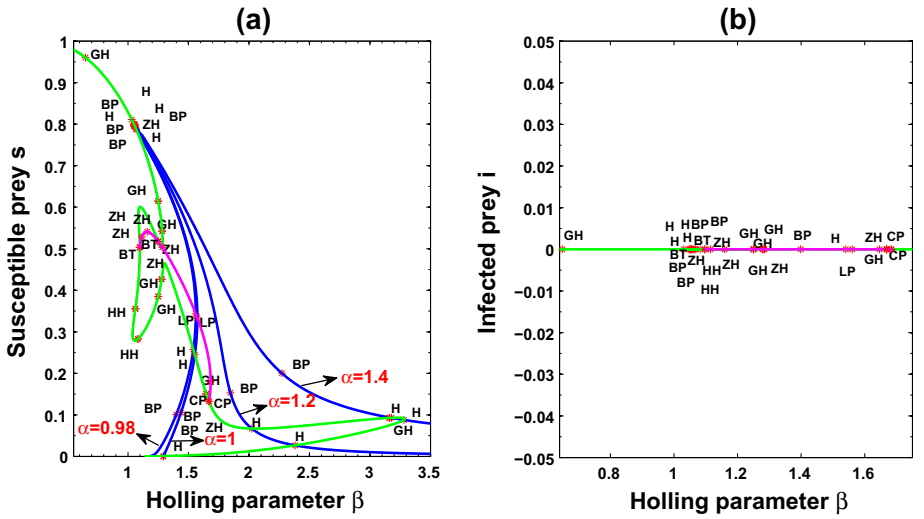

Fig. 8. Continuation curves of equilibrium from limit point (LP) with the variation of the parameter β of the (a) susceptible prey s and (b) Infected prey i. It depicts the H, GH, HH, CP, LP, BT, ZH etc. points.

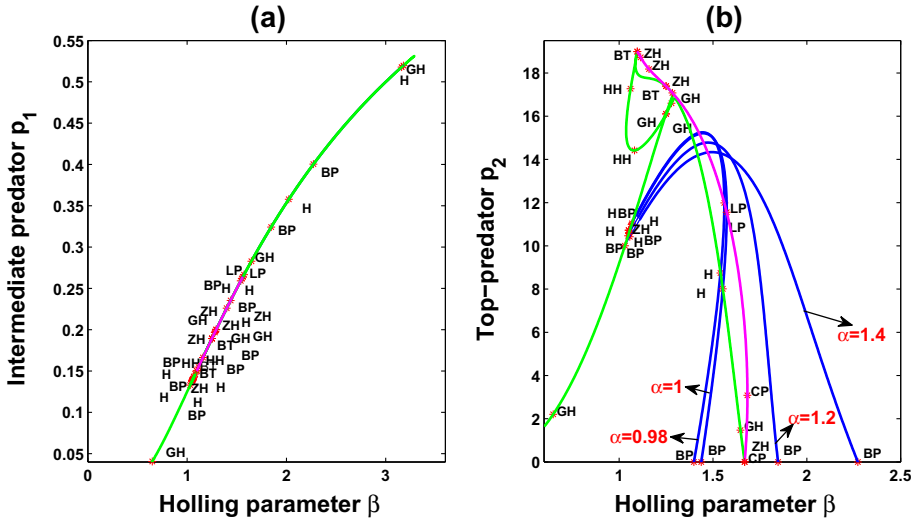

Fig. 9. Continuation curves of equilibrium with the variation of the parameter β of the (a) Intermediate predator p_1 and (b) Top-predator p_2. It depicts the H, GH, HH, CP, LP, BT, ZH etc. points.

parameters and infection rate. From Figs. 4 and 5, we observe limit cycle, period-2 to period-7 and chaotic dynamics. The global stability behaviour of the system (2) with different initial conditions is presented in Fig. 6 for different Holling parameter values α and β. Therefore, oscillatory as well as stability nature of the diseased prey population can be captured for a range of Holling parameter values. Das et al. [28] observed chaotic dynamics of the system (2) for $a = 1.15$, the period-doubling for $a = 1.17$, the limit cycle oscillation for $a = 1.2$ and finally stable steady state distribution of all four species for $a = 1.3$ for a particular value of $\alpha = 1$ and $\beta = 1$ using above set of parameter values. Here we have investigated the dynamics for $a = 1.15$ with different Holling interactions through bifurcation analysis.

7.1. Equilibrium and fold continuation

The main goal of this section is to study the pattern of bifurcation that takes place as we vary the parameters α and β. This is actually done by studying the change in the eigenvalue of the Jacobian matrix and also following the continuation algorithm. To start with we consider a set of fixed point initial solution, $s_0 = 0.77674048,\ i_0 = 2.04127 \times 10^{-128},\ p_{10} = 0.151012$

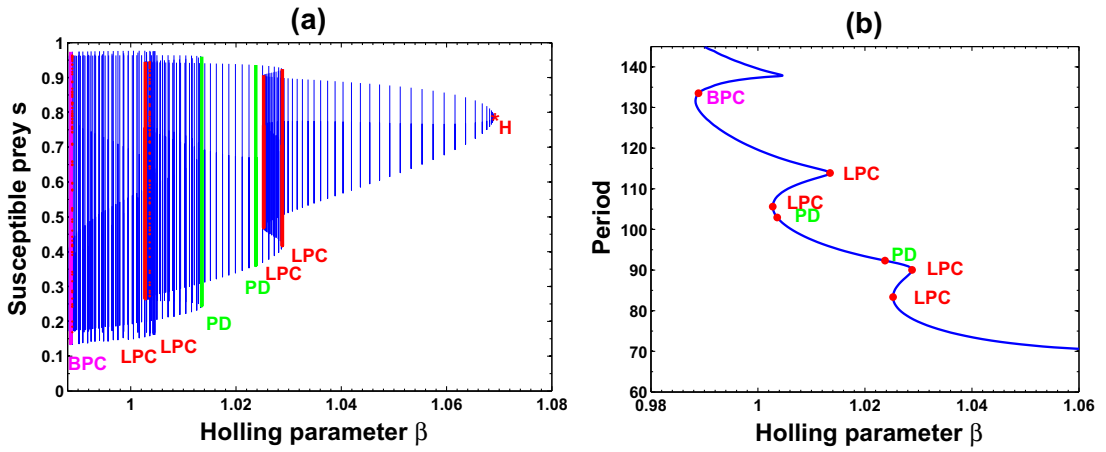

Fig. 10. (a) Family of limit cycles bifurcating from the Hopf point (H) for $\beta = 1.068978$. (b) Period of the cycle as a function of β. It depicts LPC, PD, BPC points with the variation of β.

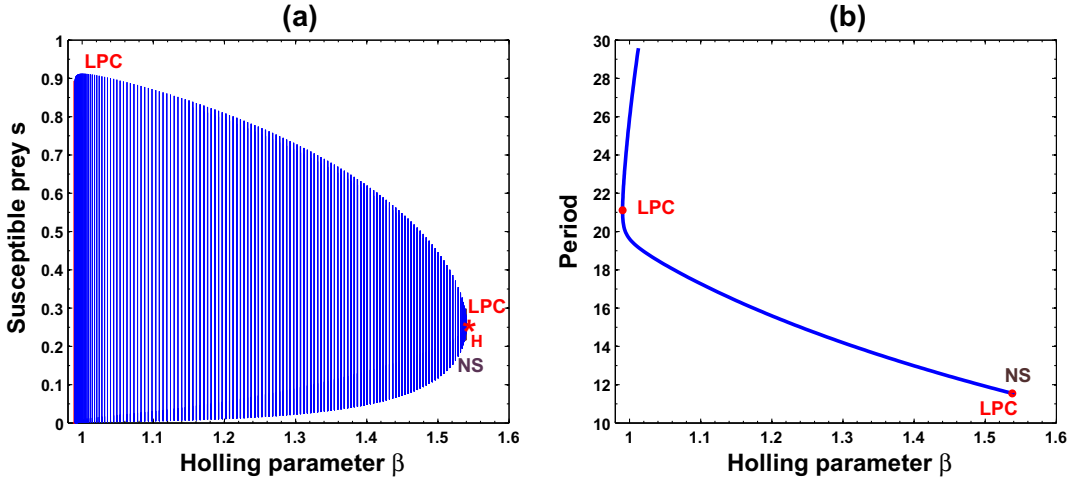

Fig. 11. (a) Family of limit cycles bifurcating from the Hopf point (H) for $\beta = 1.540269$. (b) Period of the cycle as a function of β. It depicts LPC, NS points with the variation of β.

and $p_{20} = 11.30064$, corresponding to a parameter set of values $a = 1.15,\ b = 5,\ d = 3,\ e = 0.5,\ f = 5,\ g = 2.5,\ h = 0.1,\ m = 2,\ j = 0.4,\ k = 0.1,\ l = 0.01,\ c = 3$, most of which are taken from Hastings and Powell model [43]. The characteristics of Hopf point, the limit cycle and the general bifurcation may be explored using the software package MATCONT. This package is a collection of numerical algorithms implemented as a MATLAB toolbox for the detection, continuation and identification of limit cycles. In this package we use prediction–correction continuation algorithm based on the Moore–Penrose matrix pseudo inverse for computing the curves of equilibria, limit point (LP), along with fold bifurcation points of limit point (LP) and continuation of Hopf point (H), etc.

To start with we show in Fig. 7(a) the continuation curve from the equilibrium point with β as the free parameter. In the Fig. 7(a) we get two Hopf points (H), one limit point (LP) and two branch point (BP) of s with respect to β for fixed $\alpha = 0.98$. The first Hopf point is located at $(s, i, p_1, p_2, \beta) \equiv (0.787046, 0000000, 0.142950, 11.042450, 1.068978)$. For this Hopf point the first Lyapunov coefficient turns out to be -0.1726285, indicating a supercritical Hopf bifurcation. It being negative implies that a stable limit cycle bifurcates from the equilibrium when this looses stability. The branch points (BP) occur at $\beta = 1.051086$ and at $\beta = 1.398560$. As the parameter is increasing, second Hopf point situated at $(s, i, p_1, p_2, \beta) \equiv (0.257371, 000000, 0.259227, 8.744051, 1.540269)$. For this second Hopf point the first Lyapunov coefficient turns out to be -3.898144, indicating a supercritical Hopf bifurcation. The limit point is located at $(s, i, p_1, p_2, \beta) \equiv (0.343108, 000000, 0.263828, 11.985347, 1.560608)$ with the eigenvalues as $(-0.896911, -0.056442 \pm 0.520142i, 0)$. The real part being negative, indicates that the LP is stable. The continuation curve of equilibrium point of s is also shown in same Fig. 7(a) for $\alpha = 1, 1.2, 1.4$.

Now it should be recapitulated that we have started with two parameters α and β as bifurcation parameters. To start with we show in Fig. 7(b) the continuation curve from the Hopf (H) point with respect to β. We observe six generalized Hopf (GH)

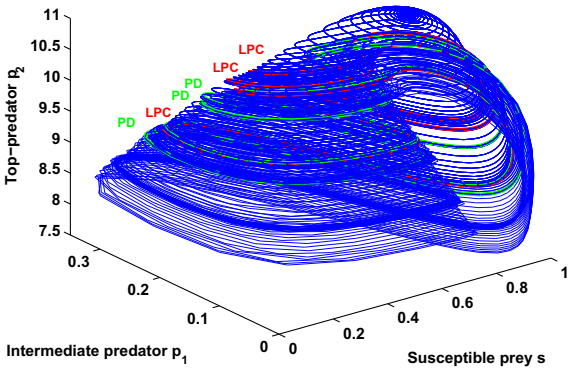

Fig. 12. Family of limit cycle bifurcating from the first Hopf point H (at $\beta = 1.068978$) with the variation of the parameter β.

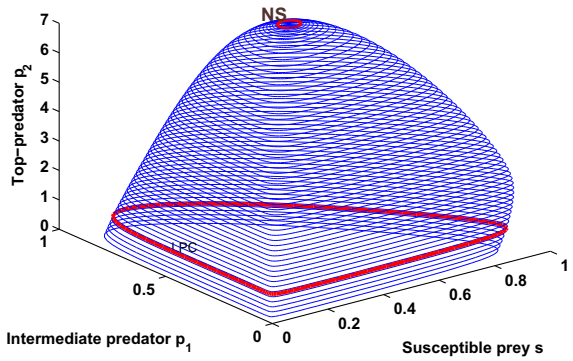

Fig. 13. Family of limit cycle bifurcating from the second Hopf point H (at $\beta = 1.540269$) with the variation of the parameter β.

points, one Bogdanov–Takens (BT) point, one zero-Hopf (ZH) point, two Neutral saddle (HH) point at different values of α and β. At the generalized Hopf (GH) points, where the first Lyapunov coefficient vanishes indicating that all GH points are non-degenerate, since the second Lyapunov coefficients are non-zero. The Bogdanov–Taken points are common points for the limit point curves and curves corresponding to equilibria with eigenvalues $\lambda_1 + \lambda_2 = 0, \lambda_3 \neq 0$. Actually, at each BT point, the Hopf bifurcation curve (with $\lambda_{1,2} = \pm i\omega, \omega > 0$) turn into the neutral saddle curve (with real $\lambda_1 = -\lambda_2$). Now, we start LP point continuation from a Bogdanov–Taken (BT) point. If we choose β and α as free parameters and start from the BT point, the continuation curve shows two BT points and two cusp points (CP) which is shown in Fig. 8(a). A similar analysis can also be carried out for the variables i, p_1 and p_2, the results being displayed in Fig. 8(b), Fig. 9(a) and Fig. 9(b) respectively.

To proceed further we start from the Hopf point (H) in Fig. 7(a) as the initial point for $\beta = 1.068978$ with fixed $\alpha = 0.98$, and get a family of stable limit cycles bifurcating from this Hopf point. This phenomenon is shown in Fig. 10(a), where again the Holling parameter β in the system is the only free parameter. One observes that at $\beta = 1.025252$, we have a LPC point with period 83.36766. At this situation two cycles collide and disappears. The critical cycle has a double multiplier equal to 1. From this it follows that a stable branch occurs after the LPC point. For $\beta = 1.028799$, another LPC point occurs with one of the multiplier is greater than 1 which indicates that the cycle is unstable after LPC point. At $\beta = 1.023759$ there is a period doubling (PD) with period 92.32825, two of the multiplier is equal to 1. However, for $\beta = 1.003603$, we observe PD again with period 102.9418, one of the multiplier is greater than 1. At $\beta = 1.002767$ and $\beta = 1.013483$, LPC's are observed with period 105.6208 and 113.8772 respectively. For $\beta = 0.9888908$, we have a branch point cycle (BPC) with period 133.5280. If we choose β and period of the cycles as free parameters and start from the Hopf point (H), as shown in Fig. 7(a), then the corresponding variation of period versus β is shown in Fig. 10(b). The similar analysis is done starting from the second Hopf point (H) as initial point, as shown in Fig. 7(a) at $\beta = 1.540269$, and we observe family of stable LPC in Fig. 11(a). The variation of period versus β is shown in Fig. 11(b). The corresponding scenario for s, p_1 and p_2 is exhibited in Figs. 12 and 13.

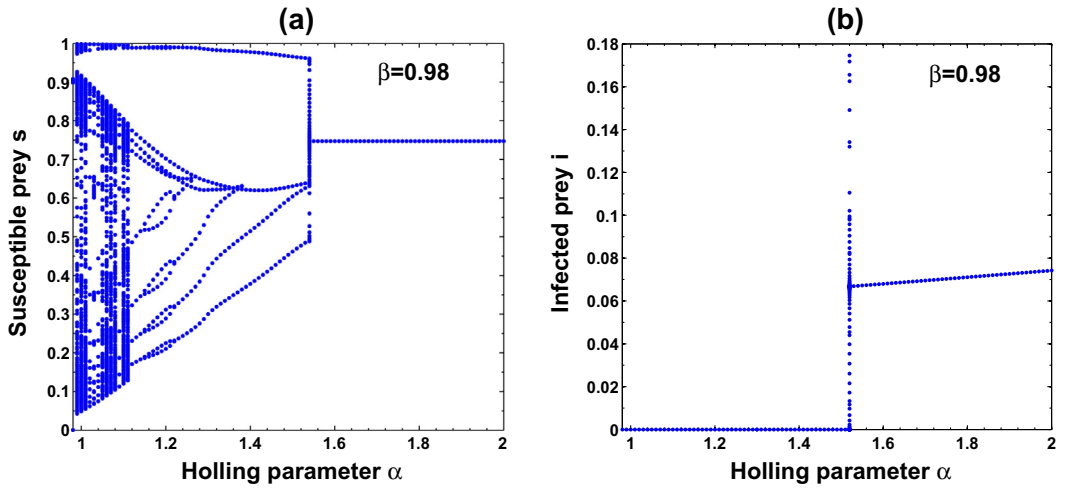

Fig. 14. Bifurcation diagram of Susceptible and Infected prey of the system (2) with respect to $\alpha \in [0.98, 2]$ taking $\beta = 0.98, a = 1.15$.

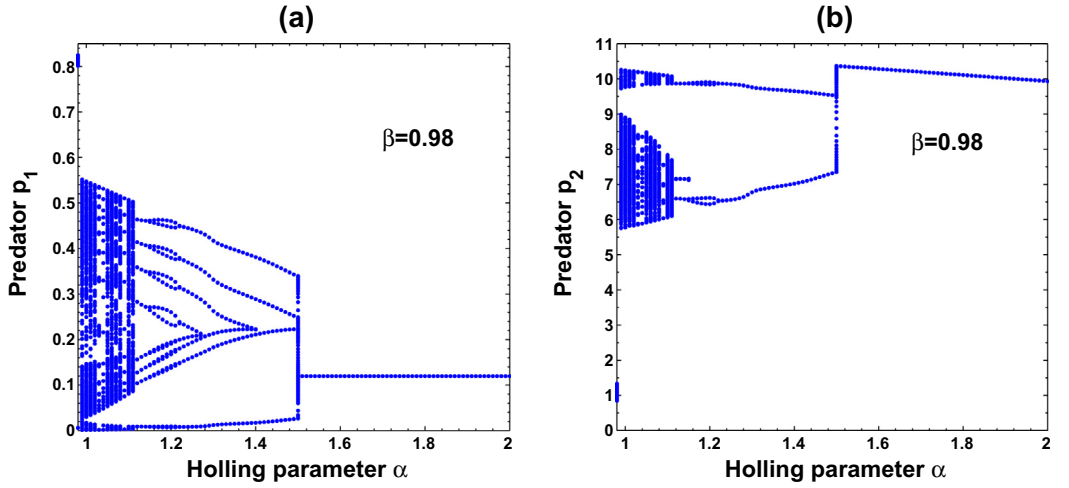

Fig. 15. Bifurcation diagram of Intermediate predator (p_1) and Top-predator (p_2) of the system (2) with respect to $\alpha \in [0.98, 2]$ taking $\beta = 0.98, a = 1.15$.

Our above analysis shows that a rich bifurcation structure exists for the predator–prey system with different Holling interactions, when α and β are varied over a wide range of values. It is to be noted that these two parameters represent two important physical quantities in the actual situation, respectively, biological pest control and agricultural research field. As such it may happen that such changes in behaviour may manifest in experimental studies also and so we need further extension of this studies.

7.2. Bifurcation

Bifurcation is an important tool to study the behaviour of a dynamical system. In this section, we study the dynamical behaviour of the system through bifurcation analysis with respect to α, β and a as free parameters taking a parameter set of values $b = 5,\ d = 3,\ e = 0.5,\ f = 5,\ g = 2.5,\ h = 0.1,\ m = 2,\ j = 0.4,\ k = 0.1,\ l = 0.01,\ c = 3$.

We have done bifurcation analysis of the system (2) with respect to Holling parameter α within the range $0.98 \leqslant \alpha \leqslant 2$, while another Holling parameter $\beta = 0.98$ and infection rate $a = 1.15$ are kept fixed. Bifurcation diagrams are presented in Figs. 14 and 15. Fig. 14(a) is the bifurcation diagram of susceptible prey of the system (2) with respect to α. The Fig. 14(a) depicts chaotic bands for $0.98 \leqslant \alpha < 1.16$, periodic oscillations for $1.16 \leqslant \alpha < 1.56$ and the system settles down to steady state after $\alpha \geqslant 1.56$. The bifurcation diagram of infected prey of the the system (2) is shown in Fig. 13(b). From Fig. 14(b), it is clear that the system becomes infection free for $0.98 \leqslant \alpha < 1.56$, but the infected prey species exists for $1.56 \leqslant \alpha \leqslant 2$. Fig. 15(a) is the bifurcation diagram of intermediate predator (p_1) with respect to Holling parameter

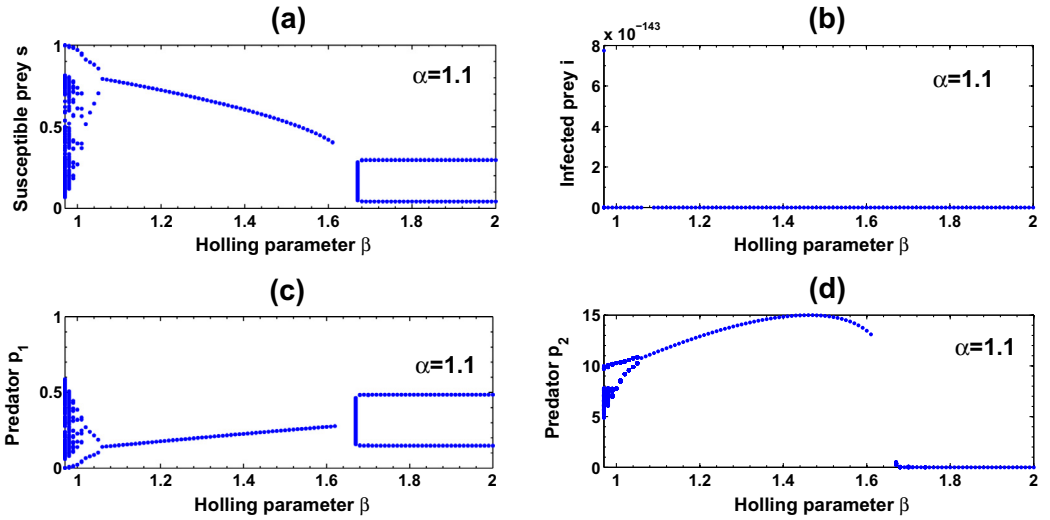

Fig. 16. Bifurcation diagram of Susceptible prey (s), Infected prey (i), intermediate predator (p_1) and top-predator (p_2) of the system (2) with respect to $\beta \in [0.97, 2]$ for $\alpha = 1.1,\ a = 1.15$.

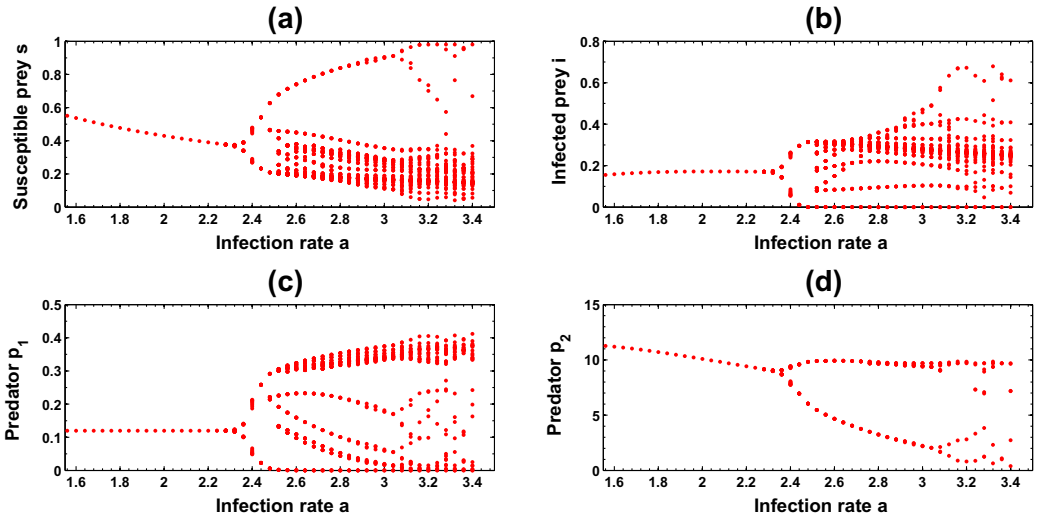

Fig. 17. Bifurcation diagram of Susceptible prey (s), Infected prey (i), intermediate predator (p_1) and top-predator (p_2) of the system (2) with respect to infection rate $a \in [2, 3.34]$ for $\alpha = 1.36, \beta = 0.98$.

$\alpha \in [0.98, 2]$. The chaotic behaviour is observed in Fig. 15(a) for $0.98 \leqslant \alpha < 1.16$. Within $1.16 \leqslant \alpha < 1.56$, we observe periodic oscillations and for $1.56 \leqslant \alpha \leqslant 2$ the system settles down to steady state. The bifurcation diagram of top-predator (p_2) with respect to α is shown in Fig. 15(b). From the Fig. 14(b) it is evident that the system has chaotic bands for $0.98 \leqslant \alpha < 1.16$, periodic oscillations for $1.16 \leqslant \alpha < 1.56$ and finally it settles down to steady state for $1.56 \leqslant \alpha \leqslant 2$.

Bifurcation analysis of the system (2) is done with respect to Holling parameter β ($0.97 \leqslant \beta \leqslant 2$) for $\alpha = 1.1$ and infection rate $a = 1.15$ with above fixed set of parameter values and it is presented in Fig. 16. From Fig. 16(a) we observe chaotic behaviour for $0.97 \leqslant \alpha \leqslant 1.06$, steady state for $1.06 < \alpha < 1.7$ and oscillatory behaviour for $1.7 \leqslant \alpha \leqslant 2$. The extinction scenario of the infected prey is shown in Fig. 16(b). Fig. 16(c) depicts chaotic behaviour for $0.97 \leqslant \alpha \leqslant 1.06$, stable state for $1.06 < \alpha < 1.7$ and oscillatory behaviour for $1.7 \leqslant \alpha \leqslant 2$. The chaotic behaviour for $0.97 \leqslant \alpha < 1.06$, stable state for $1.06 \leqslant \alpha < 1.67$ and extinction scenario of top-predator species for $1.67 \leqslant \alpha \leqslant 2$ are observed in Fig. 16(d).

One of the most important observation is that the model of Das et al. [28] with Holling type-II interaction (i.e., for $\alpha = 1,\ \beta = 1$) showed chaotic behaviour, but in this model we observe periodic behaviour for $1.16 < \alpha < 1.56$ with $\beta = 0.98$ (Fig. 14 and Fig. 15). A typical period subtracting nature of the system (2) is observed. Therefore, with the increase

of consumption rate of intermediate predator on prey stable coexistence of infected prey, susceptible prey, intermediate predator and top-predator is observed. For lower values of $\alpha < 1.56$ the consumption rate of susceptible prey is low and therefore the consumption rate of infected prey is very high (there will be no infected prey after some time) and as a result the system becomes disease free.

Here we have done bifurcation analysis of the system (2) with respect to infection rate a for $2 \leqslant a \leqslant 3.34$, taking Holling parameters $\alpha = 1.36, \beta = 0.98$ in Fig. 17. We observe steady state for $2 \leqslant a < 2.36$, periodic oscillations for $2.36 \leqslant a \leqslant 3.4$ and after $a > 3.4$, it shows chaotic behaviour. Therefore, for low infection rate population remain steady but with the increase of infection rate oscillatory nature become prominent. From Fig. 17(b) and Fig. 17(c), we notice that infected prey and intermediate predator have extinction possibility for $2.44 < a < 3.4$, whenever susceptible prey and top-predator have no such extinction risk [Fig. 17(a), Fig. 17(d)]. A typical period adding cascade nature is observed here.

8. Conclusions

A diseased food chain model with general Holling type interaction is proposed and the effects of different types of general Holling interactions are investigated. We derive sufficient conditions for local stability of equilibrium points. We also analyse the permanence and impertinence conditions of the system. The conditions for global stability are also obtained for different Holling parameters. We have explored the detailed bifurcation scenario of the proposed system varying the interaction function parameters α and β. The interesting outcomes are the occurrence of various kinds of bifurcation points in the process of continuation. Altogether our analysis reveals the internal complexity of the system in detailed manner. Bifurcation analysis shows that the dynamics of susceptible prey, infected prey, intermediate predator and top-predator are highly effected by the force of infection a as well as the interaction parameters α and β, which is in sharp contrast with the existing results [24–26]. From the simulation results, it is clear that the infected prey extinct for proper choice of interaction functions. Therefore, a diseased system reduces to a disease free system with proper choice of general Holling parameters. Therefore, we can succesfully control a disease by controlling interaction function from outside in ecosystem. We observe various types of non-unique bifurcation diagrams with respect to bifurcation parameters α, β and a respectively, having stable fixed point, limit cycle, period-2 to higher periodic oscillations, chaotic bands etc. We notice that the infected prey may survive in the system for some range of values of general Holling parameters.

Das et al. [28] reported that rate of infection and body size of intermediate predator are prime factors for disappearance of chaotic dynamics observe in HP model. Our observations indicate that chaos disappear for suitable choice of interaction functions. The most important observation is that our model with Holling type-II interaction (for $\alpha = 1, \beta = 1$) shows chaotic behaviour but for $\alpha \in [1.16, 1.56]$, $\beta = 0.98$ it shows periodic behaviour. The periodic dynamical behaviour of species was reported by many researchers from the field data [44] and laboratory data [45]. Therefore, the model with Holling type-II interactions does not always realistic in ecology, because there are lots of real food chain model which are not chaotic, but depicts oscillatory coexistence. Therefore, we conclude that a realistic food chain model depends on proper choice of general Holling parameters. Novelty of our observation is that one can control an infectious disease if the interaction functions can be controlled from outside. As research extends to higher level, we must need to continue the study for construction of real food chain model with proper general Holling interactions.

Acknowledgement

We are very grateful to the anonymous reviewer for careful reading, constructive comments and helpful suggestions, which have helped us to improve the presentation of this work significantly. The research work of S. Poria is supported by the University Grants Commission (UGC), India (F. No- 8–2/2008 (NS/PE), dated 14th December, 2011).

References

[1] D. Bernoulli, Essai dune nouvelle analyse de la mortalite causee par la petite verole, Mem. Math. Phys. Acad. Roy. Sci., Paris (1766).
[2] R. Ross, The Prevention of Malaria, second ed., Murray, London, 1999.
[3] S. Ruan, D. Xiao, J.C. Beier, On the delayed Ross–Macdonald model for Malaria transmission, Bull. Math. Biol. 70 (2008) 1098–1114.
[4] Kermack, McKendrick, Contributions to the mathematical theory of epidemics, part I, Proc. Roy. Soc. Edinb. Sec. A Math. 115 (1927) 700–721.
[5] Kermack, McKendrick, Contributions to the mathematical theory of epidemics, ii-the problem of endemicity, Proc. Roy. Soc. Edinb. Sec. A Math. 138 (1932) 55–83.
[6] Kermack, McKendrick, Contributions to the mathematical theory of epidemics, iii-further studies of the problem of endemicity, Proc. Roy. Soc. Edinb. Sec. A Math. 141 (1933) 94–122.
[7] R.M. Anderson, R.M. May, Population biology of infectious diseases 1, Nature 280 (1979) 361–367.
[8] R.M. May, R.M. Anderson, Population biology of infectious diseases 2, Nature 280 (1979) 455–461.
[9] J. Bascompte, F. Rodriguez-Trelles, Eradication thresholds in epidemiology, conservation biology and genetics, J. Theor. Biol. 192 (1998) 415–418.
[10] R.M. May, R.M. Anderson, The transmission dynamics of human immunodeficiency virus (HIV), Phil. Trans. R. Soc. Lond. B 321 (1998) 565–607.
[11] J.L. Aron, R.M. May, The population dynamics of malaria. In: Anderson, R.M. (Ed.), The Population Dynamics of Infectious Diseases, The Theory and Applications, 1982, 139–179.
[12] G. Macdonald, The Epidemiology and Control of Malaria, Oxford University Press, London, 1957.
[13] R.M. Anderson, C. Fraser, A.C. Ghani, et al, Epidemiology, transmission dynamics and control of SARS: the 2002–2003 epidemic, Philos. Trans. Roy. Soc. Lond. Ser. B Biol. Sci. 359 (2004) 1091–1105.
[14] J.D. Murray, W.L. Seward, On the spatial spread of rabies among foxes with immunity, J. Theor. Biol. 156 (1992) 327–348.
[15] N. Ferguson, R.M. Anderson, Predicting evolutionary change in the influenza A virus, Nat. Med. 8 (2002) 562–563.

[16] B.T. Grenfell, A.P. Dobson, Ecology of infectious diseases in natural populations, Publications of the newton institute, 1995.
[17] P.J. Hudson et al, The Ecology of Wildlife Diseases, Oxford University Press, 2002.
[18] L. Real, R. Biek, Infectious disease modelling and the dynamics of transmission, Curr. Top. Microbiol. Immunol. 315 (2007) 33–49.
[19] S. Sinha, O.P. Misra, J. Dhar, Modelling a predator–prey system with infected prey in polluted environment, Appl. Math. Model. 34 (2010) 1861–1872.
[20] R.M. Anderson, R.M. May, The invasion, persistence and spread of infectious diseases within animal and plant communities, Philos. Trans. R. Soc. Lond. B 314 (1986) 533–570.
[21] K.P. Hadeler, H.I. Freedman, Predator–prey populations with parasite infection, J. Math. Biol. 27 (1989) 609–631.
[22] J. Chattopadhyay, O. Arino, A predator–prey model with disease in the prey, Nonlinear Anal. 36 (1999) 747–766.
[23] M. Haque, J. Chattopadhyay, Role of transmissible disease in an infected prey-dependent predator–prey system, Math. Comput. Modell. Dyn. Syst. 13 (2007) 163–178.
[24] M. Haque, E. Venturino, The role of transmissible diseases in the Holling–Tanner predator–prey model, Theoret. Popul. Biol. 70 (2006) 273–288.
[25] M. Haque, D. Greenhalgh, When a predator avoids infected prey: a model-based theoretical study, Math. Med. Biol. 27 (2010) 75–94.
[26] M. Haque, A predator–prey model with disease in the predator species only, Nonlinear Anal.: Real World Applications 11 (2010) 2224–2236.
[27] R. Bhattacharyya, B. Mukhopadhyay, On an epidemiological model with nonlinear infection incidence: local and global perspective, Appl. Math. Model. 35 (2011) 3166–3174.
[28] K.P. Das, S. Chatterjee, J. Chattopadhyay, Disease in prey population and body size of intermediate predator reduce the prevalence of chaos-conclusion drawn from Hastings–Powell model, Ecol. Complexity 6 (2009) 363–374.
[29] B. Sahoo, S. Poria, Disease control in a food chain model supplying alternative food, Appl. Math. Model. 37 (2013) 5653–5663.
[30] M. Haque, S. Rahman, E. Venturino, Comparing functional responses in predator-infected eco-epidemics models, 2013. http://dx.doi.org/10.1016/j.biosystems.2013.06.002.
[31] A. Dhooge, W. Govaerts, Y.A. Kuznetsov, MATCONT: a Matlab package for numerical bifurcation analysis of ODEs, ACM Trans. Math. Softw. 29 (2003) 141–164.
[32] W. Mestrom, Continuation of limit cycles in MATLAB, Mathematical Institute, Master thesis, Utrecht University, The Netherlands, 2002.
[33] A. Riet, A continuation toolbox in MATLAB Mathematical Institute, Master thesis, Utrecht University, The Netherlands, 2000.
[34] T. Gross, W. Ebenhoh, U. Feudel, Enrichment and foodchain stability: the impact of different forms of predator–prey interaction, J. Theor. Biol. 227 (2004) 349–358.
[35] B. Sahoo, S. Poria, Oscillatory coexistence of species in a food chain model with general Holling interactions, Differ. Equ. Dyn. Syst. http://dx.doi.org/10.1007/s12591-013-0171-9.
[36] B. Sahoo, A predator–prey model with general Holling interactions in presence of additional food, Int. J. Plant Res. 2 (2012) 47–50.
[37] M. Nagumo, Uber die Lage der Intergralkurven gew onlicher Differentialgle ichungen, Proc. Phys. Math. Soc. Jpn. 24 (1942) 551–559.
[38] H. Freedman, P. Waltman, Persistent in models of three interacting predator–prey populations, Math. Biosci. 68 (1984) 213–231.
[39] R. Kumar, H. Freedman, A mathematical model of facultative mutualism with populations interacting in a food chain, Math. Biosci. 97 (1989) 235–261.
[40] G.J. Butler, H. Freedman, P. Walteman, Uniformly persistent systems, Proc. Am. Math. Soc. 96 (1986) 425–429.
[41] V. Hutson, R. Law, Permanent coexistence in general models of three interacting species, J. Math. Biol. 21 (1985) 289–298.
[42] J. Hofbauer, Saturated equilibria permanence and stability for ecological systems, in: L. Groos, T. Hallam, S. Levin (Eds.), Mathematical Ecology, Proc. Teieste. World Scientific, Singapur, 1986.
[43] A. Hastings, T. Powell, Chaos in a three-species food chain, Ecology 72 (1991) 896–903.
[44] C. Elton, M. Nicholson, The ten-years cycle in numbers of the lynx in Canada, J. Anim. Ecol. 11 (1942) 215–243.
[45] E.V. Leeuwan, A.A. Jansen, P.W. Bright, How population dynamics shape the functional response in a one-predator-two-prey system, Ecology 88 (2007) 1571–1581.